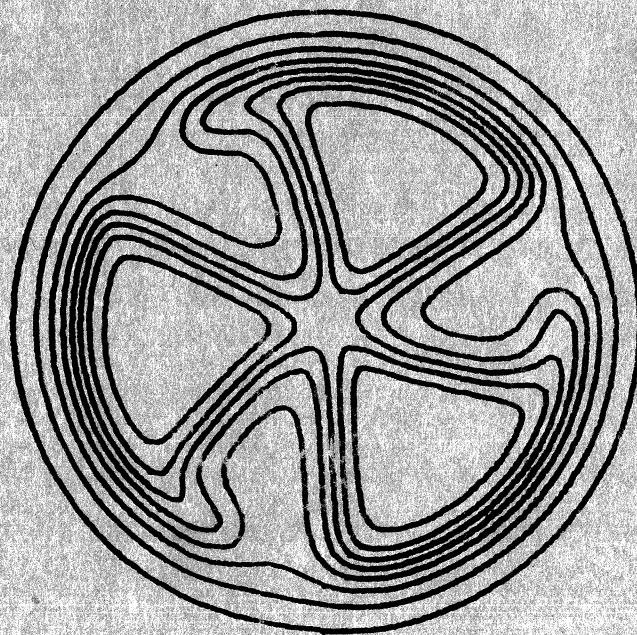


MICHIGAN STATE UNIVERSITY

CYCLOTRON LABORATORY

STUDY OF (${}^3\text{He}, t$) REACTIONS AT 70 MeV TO ISOBARIC
ANALOG STATES OF ${}^{50}\text{Cr}$, ${}^{62}\text{Ni}$, AND ${}^{90}\text{Zr}$

R. A. HINRICHS and D. L. SHOW



Study of ($^3\text{He},t$) Reactions at 70 MeV to Isobaric
Analog States of ^{50}Cr , ^{62}Ni , and ^{90}Zr *

R.A. Hinrichs and D.L. Show

Cyclotron Laboratory, Michigan State University
East Lansing, Michigan 48823

ABSTRACT

The analysis of ($^3\text{He},t$) reactions at 70 MeV to isobaric analog states of ^{50}Cr , ^{62}Ni , and ^{90}Zr have shown an energy dependence in the extracted isospin strengths consistent with results at lower energies; the interaction strengths are approximately 50% smaller than at lower bombarding energies. The shapes of the form factors in a macroscopic analysis are nuclei-dependent. A ^3He optical potential with a real strength of about 110 MeV and a volume imaginary term is strongly preferred in the ($^3\text{He},t$) calculations.

* Supported by the National Science Foundation.

I. INTRODUCTION

Charge exchange reactions to isobaric analog states (IAS) of target ground states have been studied quite extensively in recent years with both $(p,n)^{1,2}$ and $(^3\text{He},t)^{3-6}$ reactions at a variety of bombarding energies. The analysis of the differential cross sections for such reactions with the distorted wave Born approximation in a macroscopic (generalized optical potential) or microscopic (nucleon nucleon interaction) framework has yielded information on the strength and form of the isospin dependent interaction. Recent studies by Fadner, Kraushaar and Hayakawa⁶ of $(^3\text{He},t)$ transitions to IAS in several nuclei at bombarding energies between 21.4 and 37.5 MeV have shown a marked energy dependence in the extracted strength of this isospin interaction and a variation in the extracted shape of the isospin term (for the macroscopic analysis) for different nuclei. We have extended the study of $(^3\text{He},t)$ reactions to 70 MeV (the highest reported bombarding energy has been 50 MeV⁷) by examining transitions to IAS of the ground states of ^{50}Cr , ^{62}Ni and ^{90}Zr and so providing more information on the energy dependence of the charge exchange interaction.

II. EXPERIMENTAL PROCEDURE AND RESULTS

The reactions ^{50}Cr , ^{62}Ni , $^{90}\text{Zr}(^3\text{He},t)$ were studied at a bombarding energy of 70 MeV using the Michigan State University sector-focused cyclotron. The experiment was conducted in a 40°

scattering chamber with the tritons detected with a 1 cm stack of Si(Li) detectors. A $\Delta E=E$ identification program was used in conjunction with the Sigma-7 computer. An overall resolution of 150 keV was obtained, which was detector limited. The targets were all $1\text{mg}/\text{cm}^2$ rolled foils. An energy spectrum for the reaction ${}^{62}\text{Ni}({}^3\text{He},t){}^{62}\text{Cu}$ is shown in Fig. 1. At all angles the $0+$ IAS was populated significantly above the continuum, although the $2+$ excited state analog was not always observed and will not be discussed further. The excitation energies of the analog states are 0.0 MeV in ${}^{50}\text{Mn}$, 4.55 MeV in ${}^{62}\text{Cu}$ and 5.14 MeV in ${}^{90}\text{Nb}$. The experimental angular distributions for the three reactions are shown in Fig. 2. The data is quite similar for each nucleus and is characterized by small cross sections and strong oscillations.

III. ANALYSIS

DWBA calculations were carried out with the computer code DWUCK⁸ for both microscopic and macroscopic formulations.

A. Optical Model Parameters

To be as general as possible, several different sets of ${}^3\text{He}$ optical model (OM) parameters taken from several sources were used. These are listed in Table I. Except in the case of the Becchetti-Greenlees parameters⁹ (SetIV) for mass 3 projectiles, the same parameters were used for both the ${}^3\text{He}$ and triton channels.

The Becchetti-Greenlees set was established in the region $E < 40 \text{ MeV}$, $A > 40$, but their energy dependence was extended to 70 MeV. The somewhat standard OM parameters of Gibson et al.¹⁰ (Set I) have been found to possess very little target mass and energy dependences below 43 MeV; an analysis of 70 MeV elastic scattering data¹¹ has confirmed this conclusion for higher energies. The parameters of Set II (Fulmer¹²) were those for an analysis of 71 MeV ^{62}Ni elastic scattering, and the parameters of Set III (MSU) are taken from an analysis of 70 MeV ^3He elastic scattering on Ti^{50} and V^{51} .¹¹ In this last study, several families of parameters which fit the data were generated starting from the geometry of Set I. More will be said concerning these families later.

B. Macroscopic Calculations

A complex isospin-dependent potential of the form

$$\frac{1}{2} \sqrt{\frac{(N-Z)}{A^2}} \left[V f(x) + i 4 W \frac{d}{dx} f(x') \right] .$$

where $x = \frac{r - R_0}{a}$ and $f(x) = \frac{1}{1 + e^x}$

was used in the DWBA calculations. Such a form has been found to yield the best description of ($^3\text{He}, t$) data.³ The geometry for this potential was chosen to be equal to the geometry of the real and imaginary parts of the optical potential for the ^3He . The imaginary part of this asymmetry term is the dominant term in the matrix element (due to its larger radius), with the real term mainly affecting the shape of the angular distribution at backward

angles. In our calculations the relative strengths of the real to imaginary terms in the form factor were varied to provide the best possible fit for the OM set being used. Only in a few cases was it necessary to modify the geometry of the imaginary term (primarily the radius r_I) to yield a reasonable fit to the data. In general an increase in the relative strength of the real term produced an increase in the differential cross section at angles of 35° - 45° , with only negligible magnitude changes at the forward angle maxima. A larger imaginary radius tended to introduce more structure in the angular distributions, especially at backward angles.

Figure 2 shows some macroscopic calculations for ^{62}Ni , ^{90}Zr , and ^{50}Cr . In general the OM parameters of Set IV provided the best theoretical fits to the data. However with appropriate variations in the shape of the form factor, fair fits were obtained for each of the OM sets listed in Table I. For example for ^{62}Ni , OM Set II could only provide a fit with a 20% increase in the radius of the imaginary term of the asymmetry potential and with a relative strength of $V/W=5$. In all cases for ^{62}Ni , the second maximum could not be fit, while there was difficulty with the backward angle data of ^{50}Cr .

The shapes of the form factors, as characterized by the ratio of the strength of the real term to the strength of the imaginary surface-peaked term, vary over the 3 nuclei considered. This ratio of V/W is 1:9:2.7 for ^{62}Ni , ^{90}Zr , ^{50}Cr and OM Set I.

(The data of Fadner, et al.⁶ at 37.5 MeV was reanalysed to check if the same form factor used at 70 MeV still gave good fits at the lower energy. Fits to the 70 MeV data were more sensitive to the ratio of V/W.) This ratio, however, is quite sensitive to the OM parameters, and for Set IV V/W is 1:2:1 for ^{62}Ni , ^{90}Zr , ^{50}Cr .

C. Microscopic Calculations

DWBA calculations with an effective two body interaction between the projectile and target nucleons of Yukawa form and range 1.0 F were carried out for these transitions. Shell-model wavefunctions for the analog states were taken as $(f_{5/2})^2$ for ^{62}Cu , $.6(g_{9/2})^2 + .8(p_{1/2})^2$ for ^{90}Nb , and $(f_{7/2})^2$ for ^{50}Mn . (These wavefunctions were calculated in a Woods-Saxon well of geometry $r=1.25F$, $a=.65F$; a more recently used geometry of $r=1.17F$ $a=.75F$ produced a change of only 8% in the cross section.) In general the microscopic calculations were more sensitive to the OM parameters, with only certain sets giving any fit at all. Figure 3 shows calculations for ^{62}Ni , ^{90}Zr and ^{50}Cr for microscopic calculations with OM Sets III & IV. The fits are pretty good even out to backward angles except for ^{50}Cr , OM Set III. The OM parameters of Set III as listed in Table I were used in the calculations for both the ^3He and t channels while the parameters of Set IV needed the imaginary part of the triton optical potential modified by either an increase in r_I (for ^{90}Zr , $r'_I = 1.60 F$) or in W (for ^{62}Ni , $W' = 30 \text{ MeV}$ and for ^{50}Cr , $W' = 43 \text{ MeV}$) to give a good fit. The other two OM sets failed to fit the data at 70 MeV even with large changes in the triton OM parameters, although Set I did provide

an acceptable fit to the 37.5 MeV data. (Variations in the range of the Yukawa interaction from 0.7 to 1.4 F did little to change the overall structure, although there were changes in the heights of the maxima. OM Set III had a preference for $\mu=1.0$, although this was not clear for the other sets.)

From the microscopic calculations, some conclusions can be drawn regarding OM parameters, as the form factors are now the same for all sets. In ^3He elastic scattering analyses ambiguities have been noted in both the size of the real potential (family) or the form of the imaginary term. Recent studies^{13,14} indicate a potential family of 120 MeV ($r_0=1.1$ F) and a surface peaked imaginary term best describe the ^3He elastic scattering data especially when large angle scattering data is included. Different sets of OM parameters generated in fitting 70 MeV ^3He elastic data on ^{50}Ti and $^{51}\text{V}^{11}$ are listed in Table II. These cover the 110 and 170 MeV potential families with a volume or a surface-peaked form for the imaginary term. Microscopic DWBA calculations for the reactions $^{62}\text{Ni}(^3\text{He},t)$ $^{62}\text{Cu}(\text{IAS})$ were carried out with these OM parameters and are shown in Fig. 4. It is seen that a volume imaginary term (and not a surface-peaked term) is required. (It was previously noted that OM Set II provided no fits in microscopic calculations to any of the data.) It is also seen that the family of parameters with a real potential of 110-120 MeV does a better job than the set of 160-170 MeV. The fits in Fig. 3 are also in general better for Set III than for Set IV parameters for these microscopic calculations. (The Set IV family of parameters is in the same family (VR^2) as the 160-170 MeV potentials.)

IV. INTERACTION STRENGTHS

The strength of the asymmetry potential $U_1(r)$ and the projectile-nucleon interaction V_τ were obtained by a normalization between the data and DWBA calculations. These strengths were extracted in two ways: by normalization between the data and theory at the first maximum in the angular distribution ($V_1(1^{\text{st}}\text{Max})$), and by normalization between the integrated experimental and theoretical cross-sections, accounting for our finite solid angle in the latter summation (V_{TOT}). Both methods gave similar answers. The values of U_1 for ^3He bombarding energies of 70, 37.5, 29.7 and 21.4 MeV for our macroscopic calculations are shown in Fig. 5 for OM Sets I and IV where the lower energy data of Fadner et al.⁶ has been reanalysed in the same way. (Only in Set IV is there an energy dependence in the OM parameters.) For both OM sets and for all 3 nuclei, ^{62}Ni , ^{90}Zr , and ^{50}Cr , there is a marked decrease in the strength of the asymmetry term as a function of ^3He bombarding energy. Our results at 70 MeV are consistent with the trend seen at lower energies. The magnitude of the asymmetry term at 70 MeV has the average values of 7, 6 and 9 MeV for ^{62}Ni , ^{90}Zr , and ^{50}Cr , respectively. These numbers are in general a factor of two or three smaller than those found in other ($^3\text{He}, t$) work^{3,4,15} (at lower bombarding energies however).

The values of V_τ for our microscopic calculations are shown in Fig. 6 for OM Sets III and IV. Again the data of Fadner et al. has been reanalyzed with these OM sets. (A Yukawa interaction of

range 1.0 F was used.) For all 3 nuclei considered the trend again shows a decrease in the value of the isospin-dependent interaction term as a function of bombarding energy. However there are some fluctuations in V_{τ} (note ^{90}Zr for OM Set III) at different bombarding energies that make these results less conclusive than the macroscopic calculations. (It might be noted that the more consistent trends found for the microscopic analyses at the lower energies of Ref. 6 were with OM Set I, which did not fit our data very well at 70 MeV.) Our results at 70 MeV for the microscopic strengths have the average values of 18, 26, and 25 MeV for ^{62}Ni , ^{90}Zr , and ^{50}Cr respectively. Numbers found in other ($^3\text{He}, t$) work (outside of Ref. 6) are between 30 and 60 MeV (for a range of 1 F). The effective ^3He -nucleon interaction strength can be expressed in terms of the nucleon-nucleon strength by the relationship of Wesolowski et al., $^3 V_{\tau} = V_{n-n} e^{\alpha^2/1.8}$, where α is the inverse range. This yields $V_{nn} = 10$ MeV for ^{62}Ni at 70 MeV, in comparison with values of 10-20 MeV found for (p,n) studies^{2,16} at bombarding energies between 15 and 30 MeV.

Our results for the (^3He -nucleon) interaction strengths found at 70 MeV are summarized in Table III as a function of OM set used (for best fit) for ^{62}Ni and ^{90}Zr . Values from the two methods used in extracting these strengths are tabulated, as well as results of the reanalysis of 37.5 MeV data. These results again point out the decrease in the charge-exchange interaction strength at 70 MeV, relatively independent of the OM set used in the analysis.

V. SUMMARY

A study of ($^3\text{He}, t$) transitions at 70 MeV to IAS of ^{62}Ni , ^{90}Zr , and ^{50}Cr has reached the following conclusions: i) the interaction strengths extracted from both microscopic (shell model) and macroscopic (generalized optical model) calculations are approximately 50% smaller than at lower bombarding energies and dramatize the trend of the energy dependence of V_t seen there; ii) the shape of the form factor in the macroscopic calculations is different for each of the 3 nuclei, but consistent with lower energy findings; iii) in the microscopic analyses, only those calculations with optical model parameters that had a volume imaginary term fit the data. The first two conclusions are independent of the OM sets that were used, although magnitudes of the interaction strength and shapes of the macroscopic form factors are quite dependent upon the OM parameters. We can relate the conclusions concerning the energy dependence of the interaction strengths to other work, including (p,n) reactions; we summarize some of these findings in Table IV, for these results in which IAS transitions were either investigated or analysed over a range of bombarding energies. The percent decrease in the interaction strengths V_t per MeV of incident particle energy is seen to average about $2 \pm 1\%$ for all cases, including the present results. This number is significantly larger than the energy dependent decrease in the real part of the ^3He -nucleus optical potential. These results should provide additional impetus for studies into the DWBA with respect to charge-exchange reactions; two-step processes and exchange might be important in describing these energy dependent effects.

REFERENCES

1. G.R. Satchler, R.M. Drisko and R.H. Bassel, Phys. Rev. 136, B637(1964).
2. C. Wong, J.D. Anderson, J.W. McClure, B.A. Pohl, and J.J. Wesolowski, Phys. Rev. C5, 158(1972).
3. J.J. Wesolowski, E.H. Schwarz, P.G. Roos, and C.A. Ludeman, Phys. Rev. 169, 878(1968).
4. P. Kossanyi-Demay, P. Roussel, H. Faraggi, and R. Schaeffer, Nuc. Phys. A148, 181(1970).
5. F.D. Becchetti, W. Makofske, and G.W. Greenlees, to be published.
6. W.L. Fadner, J.J. Kraushaar, and S.I. Hayakawa, Phys. Rev. C5, 859(1972).
7. G.C. Ball and J. Cerney, Phys. Rev. 177, 1466(1969) and D.C. Hensley, C.D. Goodman and M.J. Saltmarsh, ORNL-4649 (1970).
8. Computer code by P.D. Kunz.
9. F.D. Becchetti and G.W. Greenlees in Polarization Phenomena in Nuclear Reactions, ed. by H.H. Barschall and W.Haeberli (1971) p. 682.
10. E.F. Gibson, B.W. Ridley, J.J. Kraushaar, M.E. Rickey, and R.H. Bassel, Phys. Rev. 155, 1194(1967).
11. R.A. Hinrichs, R.R. Doering and A. Galonsky, Bull Am. Phys. Soc. 16, 628(1971) and to be published.
12. C.B. Fulmer, private communication.
13. C.B. Fulmer and J.C. Hafele, to be published.

14. G.R. Siegel, F.B. Shull and J.C. Hafele, Bull. Am. Phys. Soc. 16, 646(1971).
15. W.L. Fadner, J.J. Kraushaar and L.C. Farwell, Nucl. Phys. A178, 385(1971).
16. A.S. Clough, C.J. Batty, B.E. Bonner and L.E. Williams, Nuc. Phys. A143, 385(1970).
17. A. Galonsky, R.K. Jolly, R. St. Onge, T. Amos, to be published.

TABLE I

OH Parameters - 70 MeV - ^{62}Ni

Set	V	r_c	a	W_V	W_D	r_I	a_I	Reference
I	170.6	1.14	.712	18.5	-	1.6	.829	Gibson ¹⁰
II	126.5	1.17	.837	-	20.4	1.26	.841	Fulmer ¹²
III	114.2	1.14	.842	18.4	-	1.62	.793	MSU ¹¹
IV ^3He :	145.	1.20	.72	22.9	-	1.40	.88	Becchetti- Greenlees ⁹
t:	152.4	1.20	.72	12.3	-	1.40	.84	

TABLE II

OM Parameters - $^{51}\text{V} + ^3\text{He}$, 70 MeV

Set	V	r_c	a	W_V	W_D	r_I	a_I	χ^2/N
A	114.2	1.14	.842	18.4	-	1.62	.793	43
B	182.2	1.14	.702	37.5	-	1.21	1.16	88
C	120.1	1.14	.816	-	18.6	1.28	.805	16
D	180.8	1.14	.710	-	25.7	1.03	.980	71

TABLE III

Interaction Strengths

OM Set	V_{TOT}		$V_1(1^{st}Max)$	
	70 MeV	37.5 MeV	70 MeV	37.5 MeV
I (V=W)	8.4 MeV	13.3 MeV	4.9 MeV	12.4 MeV
IV (V=W)	10.	22.	6.8	21.
II (Macro)	8.9	17.	9.4	17.
IV (Micro)	11.	29.	18.	27.
III (Micro)	17.	33.	18.	35.
I (V=9W)	3.5	13.	3.7	11.
IV (V=2W)	7.9	41.	7.8	32.
II (Macro)	4.8	18.	4.5	14.
IV (Micro)	25.	63.	26.	48.
III (Micro)	34.	39.	33.	26

 $^{62}_{Ni}$ $^{90}_{Zr}$

TABLE IV

Interaction Strengths - Summary

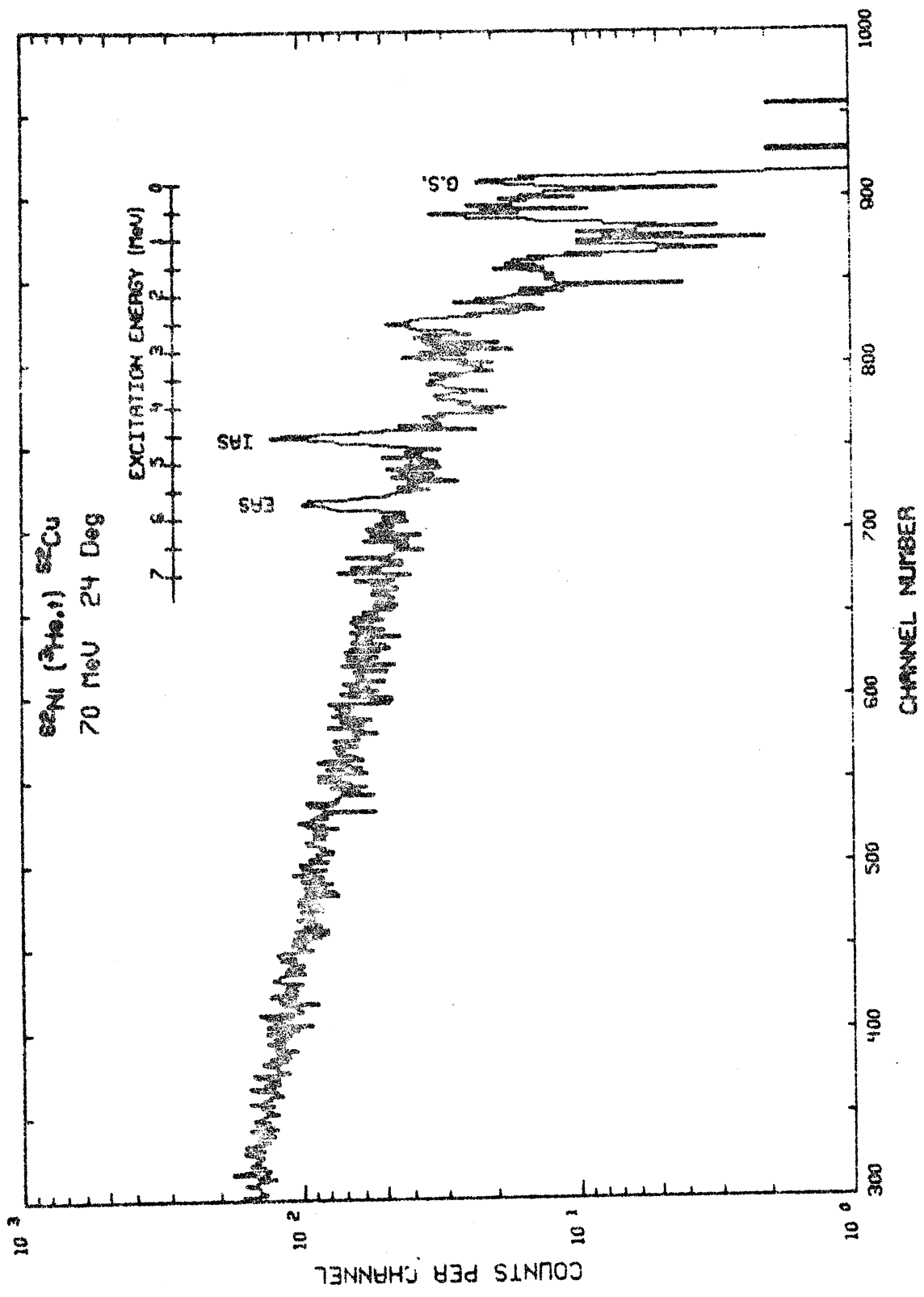
Source	Targets	Particle and Energies (MeV)	% decrease in V_T / MeV particle energy
Present MSU + Fadner ⁶	Ni, Zr	³ He, 21-70	1-2%
Galonsky ¹⁷	Al, Zr	p, 22-40	1-1/2-2%
Becchetti ⁵	Ni	³ He, 25-37	2-1/2%
Clough ¹⁶	lp shell	p, 30-50	3%
Wong ²	Al-Pb	p, 17-50	1-1/2%

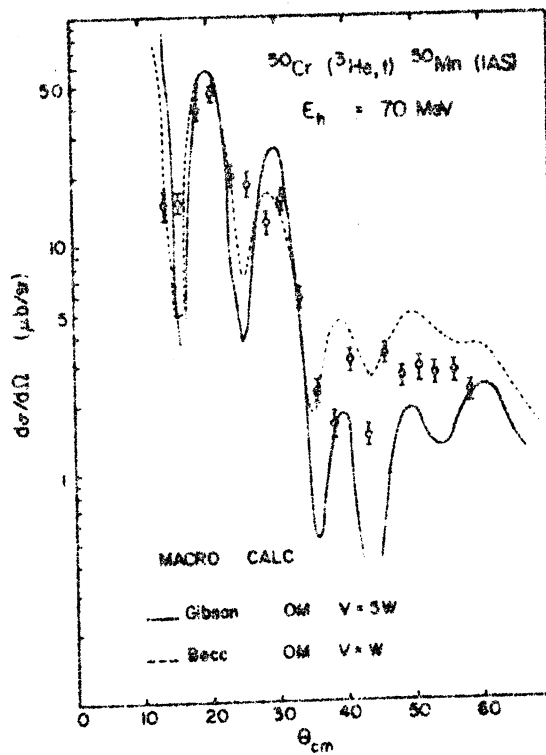
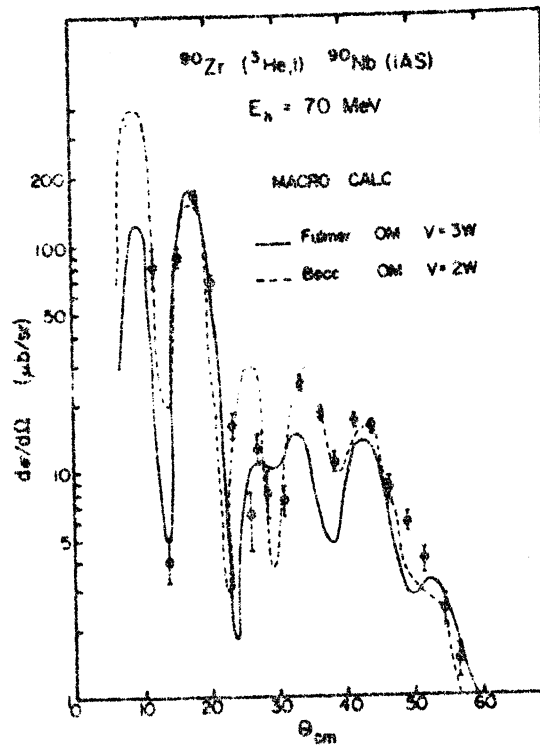
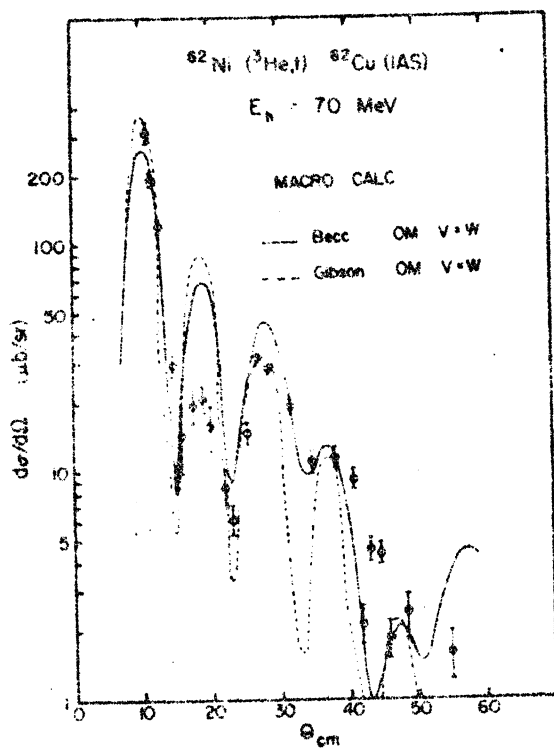
FIGURE CAPTIONS

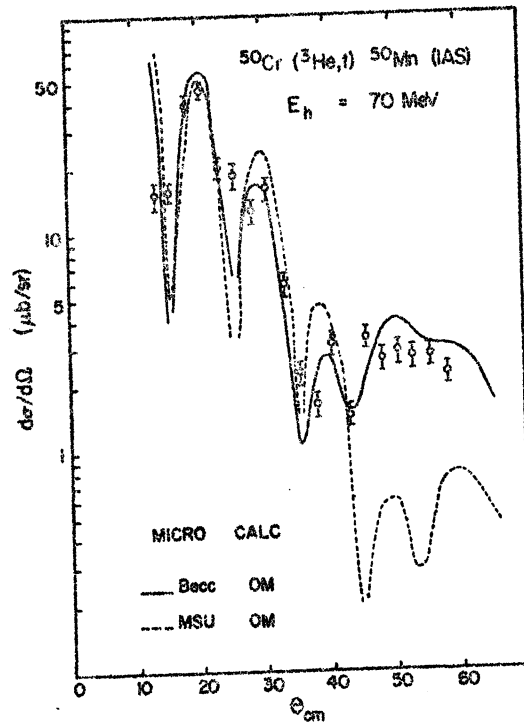
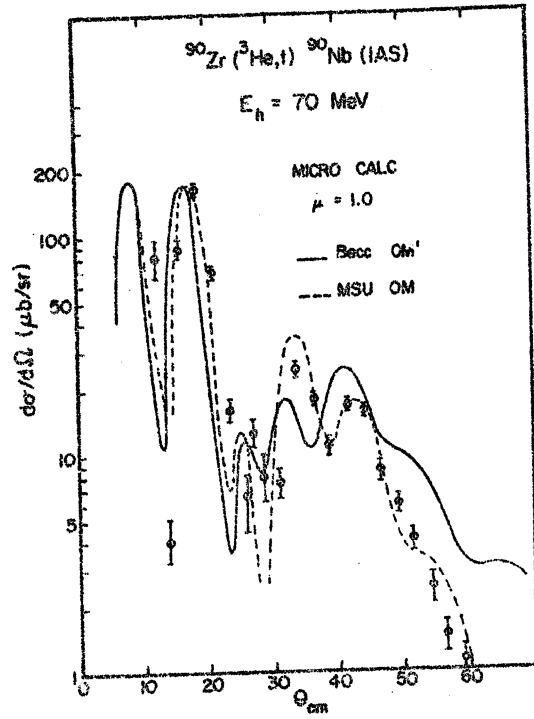
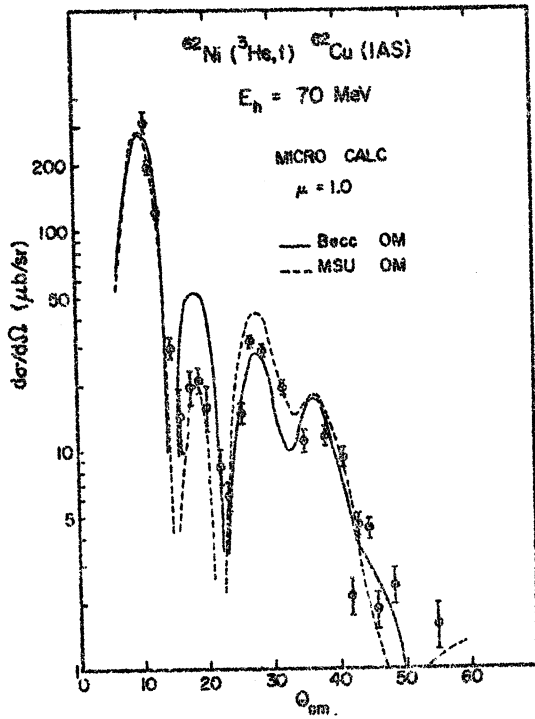
- Fig. 1 Energy spectrum for the reaction $^{62}\text{Ni}(^3\text{He},t)^{62}\text{Cu}$ at 24° . The isobaric analogs of the ground state (IAS) and first excited state (EAS) of ^{62}Ni are noted.
- Fig. 2 Angular distributions for $(^3\text{He},t)$ reactions at 70 MeV to the isobaric analogs of the ground states of ^{62}Ni , ^{90}Zr and ^{50}Cr . The curves shown are DWBA calculations with a complex macroscopic form factor (with noted relative amounts of real and imaginary strengths) for the OM parameter sets of Table I.
- Fig. 3 Angular distributions for $(^3\text{He},t)$ reactions at 70 MeV to the isobaric analogs of the ground states of ^{62}Ni , ^{90}Zr and ^{50}Cr . The curves shown are microscopic DWBA calculations (normalized to the data) with simple shell model wave functions and a Yukawa force of range 1.0 F.
- Fig. 4 Angular distributions for the reaction $^{62}\text{Ni}(^3\text{He},t)^{62}\text{Cu}$ (IAS). The curves shown are DWBA calculations (Normalized at the first maximum) with a microscopic form factor (Yukawa form, range 1.0 F) with different types of OM potentials as listed in Table II.
- Fig. 5 Strength of the Asymmetry Potential extracted from the present 70 MeV $(^3\text{He},t)$ data on ^{62}Ni , ^{90}Zr and ^{50}Cr and that of Ref. 6 at 37.5 and 21.4 MeV for calculations with a macroscopic form factor (with shapes as described in the text but the same at each energy) for OM Sets I

and IV. The dashed lines are only to guide the eye. The error bars correspond to about a 10% uncertainty in the extraction of U_1 due to statistical errors in the data and judgements in the normalization between theory and experiment.

Fig. 6 Strength of the Microscopic Interaction V as a function of ^3He bombarding energy for OM Sets III and IV. See caption for Fig. 5.







$^{62}\text{Ni}({}^3\text{He}, t){}^{62}\text{Cu}$ (IAS)

$E_n = 70$ MeV

MICRO CALC

OM	SET	V	W
A	—	114	voi.
C	- - -	120	surf
D	- . - .	180	surf

